4th IASPEI / IAEE International Symposium:

Effects of Surface Geology on Seismic Motion

August 23–26, 2011 · University of California Santa Barbara

NUMERICAL MODELING OF LIQUEFACTION EFFECTS

Ross W. Boulanger
University of California
Davis, CA 95616
USA

Ronnie Kamai
University of California
Davis, CA 95616
USA

Katerina Ziotopoulou
University of California
Davis, CA 95616
USA

ABSTRACT

Development and initial applications of a sand plasticity model for nonlinear seismic deformation analyses involving liquefaction are described. The model follows the basic framework of the stress-ratio controlled, critical state compatible, bounding surface plasticity model for sand presented by Dafalias and Manzari (2004). Modifications were implemented to improve its ability to approximate stress strain responses important to geotechnical earthquake engineering applications. Initial applications of the model have included one-dimensional site response analyses of down-hole arrays where liquefaction was triggered and two-dimensional analyses of dynamic centrifuge model tests involving liquefaction and lateral spreading. An overview of the sand model is presented, followed by example results from these initial validation studies.

INTRODUCTION

Numerical modeling of liquefaction effects is performed in practice and research using a wide range of constitutive models and numerical procedures. The constitutive models vary in complexity, depending on which aspects and details of liquefaction behavior they are intended to approximate. For example, there are uncoupled total-stress models that track cyclic stresses for determining when to trigger liquefaction and impose a residual strength; these types of phenomenological models may be useful for evaluating how liquefaction-induced strength loss affects stability or deformations of a structure, but are not capable of simulating realistic stress-strain behaviors and thus cannot generate responses which arise from those behaviors. Coupled, effective-stress models can provide more realistic simulations of stress-strain behaviors, but they often require considerably more engineering effort for calibration and use. Simulation results can also be significantly affected by the details of the numerical procedures, such as the specification of boundary conditions, input motions, numerical damping, pore water flow, and mesh geometry updating. Consequently, there is a need in practice to further develop constitutive models that provide realistic approximations of soil behavior while being easy to use, and to develop more standardized protocols for the calibration and validation of constitutive models and numerical modeling procedures.

In this paper, the development and initial applications of a sand plasticity model for numerical modeling of liquefaction effects are described. The sand plasticity model, PM4-Sand, is a stress-ratio controlled, critical state compatible, bounding surface plasticity model that follows the basic framework by Dafalias and Manzari (2004) with modifications that improve its ability to approximate stress strain responses important to geotechnical earthquake engineering applications. The motivation behind the model, its basic formulation, and examples of its constitutive responses are presented. Initial applications of the PM4-Sand model have included one-dimensional site response analyses of down-hole arrays where liquefaction was triggered and two-dimensional analyses of dynamic centrifuge model tests involving liquefaction and lateral spreading. Example results are presented from the site response analyses of the Wildlife Liquefaction Array during the 1987 Superstition Hills Earthquake and from two-dimensional analysis of a dynamic centrifuge model test by Kamai et al. (2008).

PM4-SAND PLASTICITY MODEL

Development of the PM4-Sand model was guided by the need in practice for models that can reasonably approximate, and be quickly

calibrated to, the engineering design relationships that are commonly used for estimating the stress-strain behaviors of liquefiable soils. Stress-strain behaviors that can be important for applications include the following items.

- The cyclic resistance ratio (CRR) against triggering of liquefaction, which is commonly estimated based on SPT and CPT penetration resistances with case-history-based liquefaction correlations. The CRR is the cyclic stress ratio (e.g., CSR = τ_{cyc}/σ'_{vc}, with τ_{cyc} = horizontal cyclic shear stress, σ'_{vc} = vertical consolidation stress) that is required to trigger liquefaction in a specified number of equivalent uniform loading cycles.
- The response under the irregular cyclic loading histories produced by earthquakes, which is approximately represented by the relationship between CRR and number of equivalent uniform loading cycles. This aspect of behavior also directly relates to the magnitude scaling factors (MSF) that are used with liquefaction correlations in practice.
- The dependence of CRR on effective confining stresses and sustained static shear stresses. These aspects of behavior are represented by the K_σ and K_α correction factors, respectively, that are used with liquefaction correlations in practice.
- The accumulation of shear strains after triggering of liquefaction. Evaluations of reasonable behavior are often based on comparisons to laboratory tests results for similar soils in the literature.
- The strength loss as a consequence of liquefaction, which may involve explicitly modeling phenomena such as void redistribution or empirically accounting for it through case history-based residual strength correlations.
- The small-strain shear modulus which can be obtained through in-situ shear wave velocity measurements.
- The shear modulus reduction and equivalent damping ratio relationships prior to triggering of liquefaction. These aspects of behavior are commonly estimated using empirical correlations derived from laboratory test results for similar soils.
- The drained and undrained monotonic shear strengths, which may be estimated using correlations to SPT and CPT penetration resistances.
- The volumetric strains during drained cyclic loading or due to reconsolidation following triggering of liquefaction, both of which may be estimated using empirical correlations derived from laboratory test results for similar soils.

The utility of a nonlinear soil model in practice is dependent on: (1) its ability to approximate the above behaviors over a broad range of conditions and, (2) the level of engineering effort required for calibrating the model. For example, a single geotechnical structure can have strata or zones of sand ranging from very loose to dense under a wide range of confining stresses, drainage conditions, and loading conditions, such that the engineering effort is greatly reduced if the constitutive model can reasonably approximate stress-strain behaviors under all these conditions. If the model cannot approximate the trends across all these conditions, then extra engineering effort is required by the need to decide what behaviors should be prioritized in the calibration process, and sometimes by the need to repeat the calibrations for the effects of different initial conditions within the same geotechnical structure.

Model Formulation

The PM4-Sand model follows the basic framework of the stress-ratio controlled, critical state compatible, bounding-surface plasticity model for sand presented by Dafalias and Manzari (2004). On a q-p′ space, the model has a narrow stress-ratio based elastic cone and three other key surfaces – the bounding, dilation and critical-state surfaces (Fig. 1). The locations of the dilation and bounding surfaces are dependent on the state of the soil (Fig. 2), such that they move towards the critical state surface in a scissor-like movement when the soil is sheared towards critical state, with all three surfaces coinciding when the soil reaches critical state.

A series of modifications and additions to the model were incorporated to improve its ability to approximate the trends observed in empirical correlations commonly used in practice. These constitutive modifications included:

- revising the fabric formation/destruction to depend on plastic shear rather than plastic volumetric strains;
- adding fabric history and cumulative fabric formation terms;
- modifying the plastic modulus relationship and making it dependent on fabric;
- modifying the dilatancy relationships to provide more distinct control of volumetric contraction versus expansion behavior;
- adding sedimentation effects for improved estimation of reconsolidation strains following liquefaction;
- providing a constraint on the dilatancy during volumetric expansion so that it is consistent with Bolton's (1986) dilatancy relationship;
- modifying the elastic modulus relationship to include dependence on stress ratio and fabric history;
- modifying the logic for tracking previous initial back-stress ratios (i.e., loading history effect);
- recasting the critical state framework to be in terms of a relative state parameter index (i.e., ξ_R in Fig. 2) rather than a state parameter;
- simplifying the formulation by restraining it to plane strain without Lode angle dependency for the bounding and dilation surfaces; and
- providing default values for all but three primary input parameters.

The constitutive equations and model behaviors are provided in Boulanger (2010).

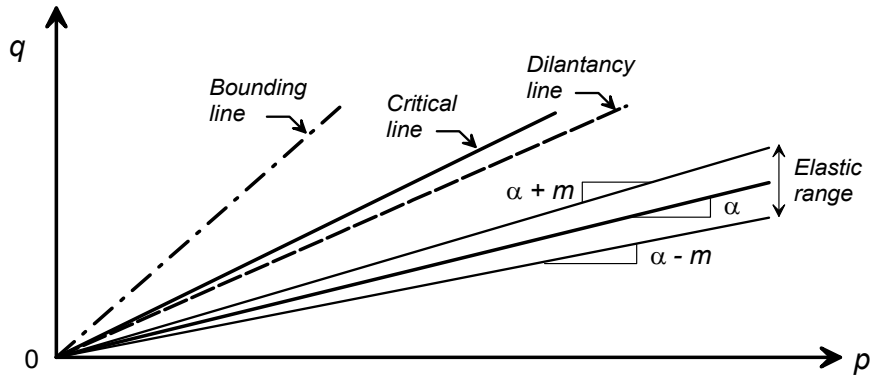

Fig. 1. Schematic of yield, critical, dilatancy, and bounding lines in q-p space (after Dafalias & Manzari 2004).

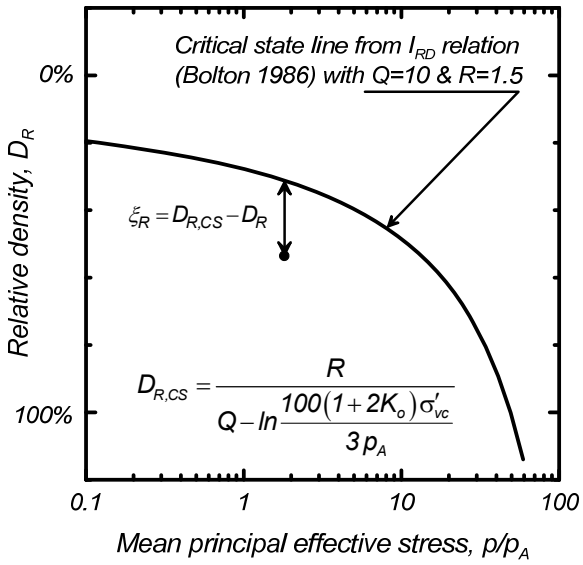

Fig. 2. Definition of the relative state parameter index, ξ_R (Boulanger 2003).

There are three primary parameters that are most important for model calibration, and a secondary set of 17 parameters that may be modified from their default values in special circumstances. The three primary model input parameters are: the shear modulus coefficient, G_o, which should be calibrated to the estimated or measured in-situ shear wave velocity; an apparent relative density (D_R) which affects the peak drained and undrained strengths and the rate of strain accumulation during cyclic loading; and the contraction rate parameter, h_{po} which is used to calibrate the model to the estimated in-situ cyclic resistance ratio. Secondary input parameters have default values that have been calibrated to produce reasonable agreement with the trends in typical design correlations, although users should still confirm through element loading calibrations that the default parameters are appropriate for their particular conditions. The secondary input parameters are described in Boulanger (2010), along with commentary on the recommended default values.

The model was implemented as a user-defined material for use with the commercial program FLAC (Itasca 2009). The simulations presented in the following section were performed using FLAC.

Example Responses

The stress-strain response of the model for undrained cyclic simple shear loading is illustrated in Fig. 3 for sand at D_R of 35%, 55%, and 75%, which correspond to SPT $(N_1)_{60}$ values of approximately 6, 14, and 26, respectively. Values for G_o were obtained using a form of the correlation by Andrus and Stokoe (2000). Values for h_{po} were obtained by calibrating the model to obtain the $CRR_{M=7.5}$ values computed using the SPT-based liquefaction triggering correlation by Idriss and Boulanger (2008). All secondary input

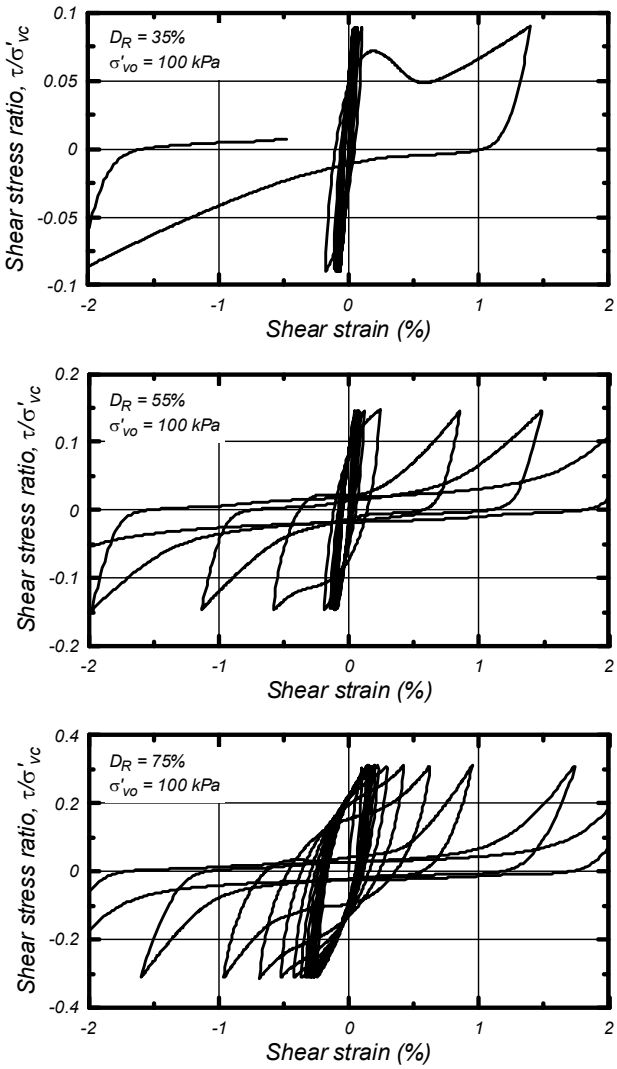

Fig. 3. Undrained cyclic DSS loading responses for D_R = 35, 55, and 75'% with a vertical effective consolidation stress of 1 atm and without any initial static horizontal shear stress.

parameters were assigned their default values. The stress-strain responses capture the cyclic mobility behavior of sands, with the progressive post-liquefaction increase in cyclic strain amplitudes being faster for the looser specimen and slower for the denser specimen.

The cyclic stress ratio (CSR) that causes a single-amplitude shear strain of 3% in undrained DSS loading is plotted versus number of uniform loading cycles in Fig. 4 for sand at D_R of 35, 55, and 75%. These results are for a vertical consolidation stress of 1 atm, an initial K_o of 0.5, and zero initial static shear stress ratio. The simulation results in this figure were fitted with a power law, for which the exponent "b" is labeled beside each curve. The slopes of these curves relating CRR to number of loading cycles are in good agreement with typical values obtained in laboratory testing studies (e.g., Liu et al. 2001, Idriss and Boulanger 2008).

The effect of overburden stress on CRR is illustrated in Fig. 5 showing the equivalent K_σ values from these simulations, where K_σ is the ratio of the CRR to the value of CRR that is obtained when the vertical consolidation stress is 1.0 atm. These K_σ values, determined at 15 uniform loading cycles, are compared in Fig. 5 to the relationships recommended by Boulanger and Idriss (2008). The simulated effects of confining stress are in good agreement with the design relationship by Boulanger and Idriss (2008), as expected because the dilatancy relationship was specifically calibrated to approximate this relationship.

Drained strain-controlled cyclic DSS loading for sand at D_R of 55% under vertical consolidation stresses of 1.0, 4.0, and 16.0 atm with K_o = 1.0 is shown in Fig. 6, with results also shown for the equivalent modulus reduction (G/G_{max}) and equivalent damping ratio

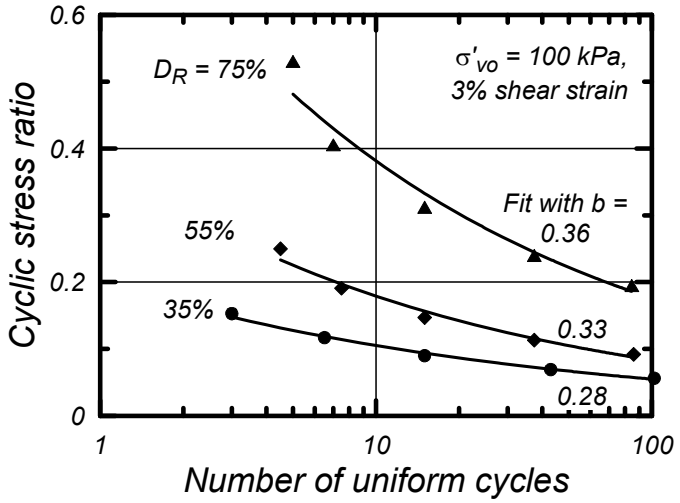

Fig. 4. .Cyclic stress ratios versus number of uniform loading cycles in undrained DSS loading causing single-amplitude shear strains of 3% for D_R = 35, 55, and 75% with a vertical effective consolidation stress of 1 atm.

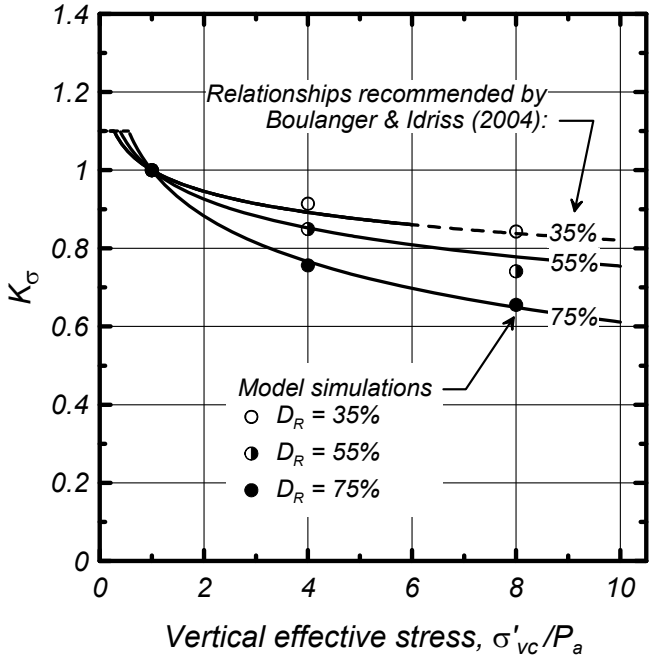

Fig. 5. Comparison of K_σ ratios from simulations versus relationships by Boulanger and Idriss (2004).

versus cyclic shear strain amplitude. Also shown are the modulus reduction and equivalent damping ratio curves recommended for sands at different depths by EPRI (1993). The simulated modulus reduction and equivalent damping ratio curves depend on the effective confining stress in a pattern and magnitude that is consistent with empirical design correlations, such as the ones proposed by EPRI (1993). The simulated modulus reduction and damping curves are in reasonable agreement with the empirical curves over a fairly broad range of shear strain amplitudes. As shown in Fig. 6, the model's response avoids the problem, common to many plasticity models, of producing excessively high equivalent damping ratios as shear strain amplitudes exceed about one percent.

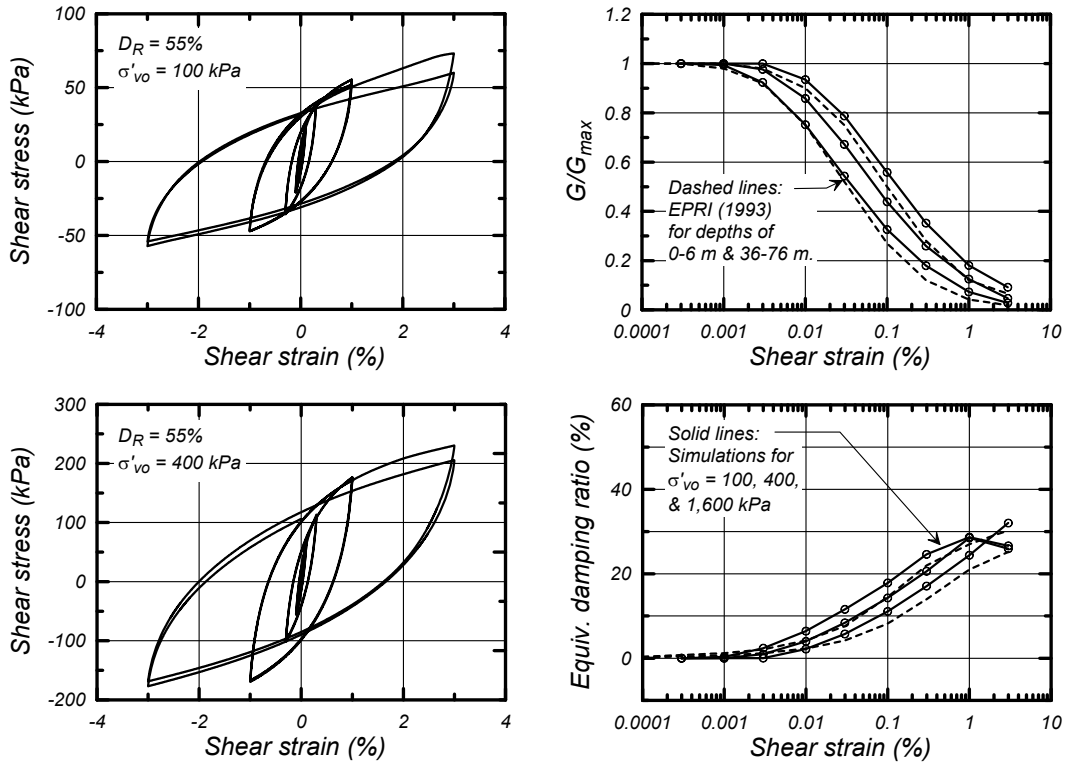

Fig. 6. Stress-strain responses and the corresponding shear modulus reduction and equivalent damping ratios from drained strain-controlled cyclic DSS loading for D_R = 55% under vertical effective consolidation stresses of 1, 4, and 16 atm.

SITE RESPONSE ANALYSES OF LIQUEFYING SITES

Two case histories of liquefaction at down-hole array stations were analyzed by Ziotopoulou (2010) using one-dimensional dynamic site response procedures and utilizing three different constitutive models for liquefiable soils. The selected case histories were the responses of the Port Island array during the 1995 Kobe Earthquake and the Wildlife Liquefaction Array (WLA) during the 1987 Superstition Hills Earthquake. The three constitutive models, which included PM4-Sand, represented a range of modeling complexity and were run as user-defined models in the finite difference program FLAC (Itasca 2009). Full details of the calibration process, input parameters, numerical procedures, and sensitivity studies are given in Ziotopoulou (2010).

For example, the profile shown in Fig. 7 for the WLA site summarizes available SPT, CPT, and V_s data (Bennett et al. 1984, Holzer and Bennett, 2010 personal communications) and indicates the depths of the strong ground motion recordings. The constitutive models for the liquefiable soils were calibrated to produce CRR values that matched those obtained using the field SPT N values and the liquefaction triggering correlation by Idriss and Boulanger (2008). Single elements were subjected to uniform cyclic, undrained, direct simple shear loading, and the h_{po} parameter was varied until the simulated CRR for 15 uniform loading cycles matched the SPT-derived value for a M = 7.5 earthquake.

Computed and recorded responses at the ground surface of the WLA for the NS component of motion are compared in Fig. 8. The acceleration time series in Fig. 8(a) is for the baseline set of properties estimated from the site characterization data, whereas the response spectra in Fig. 8(b) include results for the baseline case and cases with the shear wave velocities or cyclic resistance ratios increased and decreased by 20%. The computed horizontal accelerations at the ground surface reasonably approximate the recorded responses, including the modest acceleration spikes that occur after liquefaction has been triggered and which are associated with cyclic mobility behavior (e.g., Holzer and Youd 2007). The response spectra for the computed motions are lower than those for the recorded motion at periods greater than about 1.0 sec, but are otherwise in reasonable agreement.

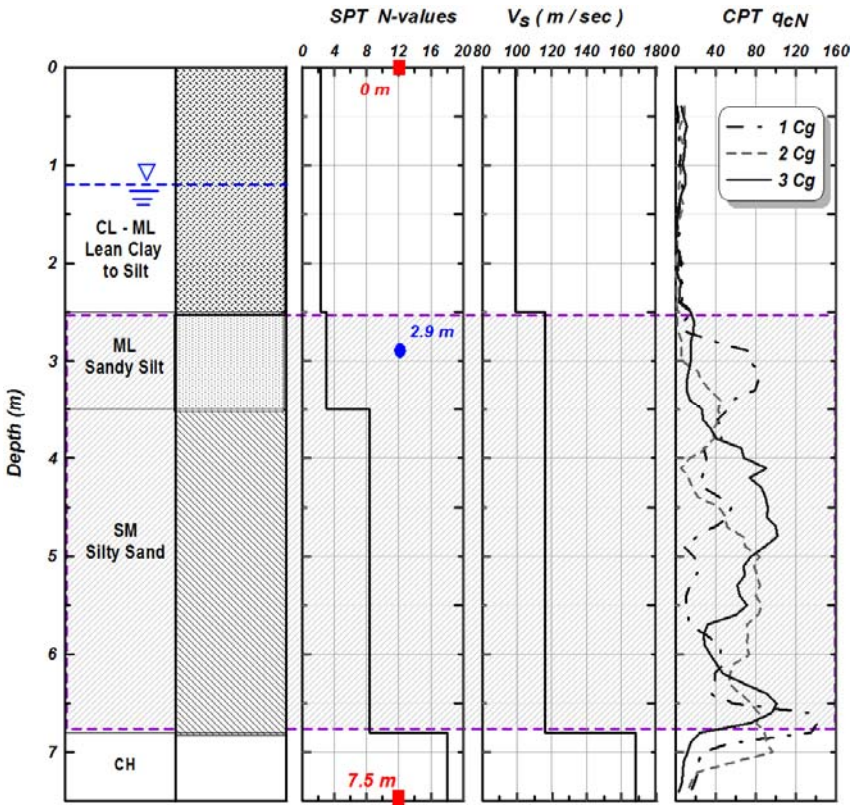

Fig. 7. Wildlife Liquefaction Array profile showing average SPT N values, shear wave velocities, CPT tip resistances, depths of recordings (accelerometers at 0 and 7.5 m; pore-pressure transducer at 2.9 m) and highlighting the liquefiable strata [data from Bennett et al. 1984, Holzer and Bennett, 2010 personal communications].

These example results are illustrative of the trends observed in the comparisons of responses for both directions of motion at the two sites, although the nature and magnitude of differences between recorded and computed responses were quite variable. The results obtained using the UBCSAND (Byrne et al. 2004) and PM4-Sand models for the liquefiable layers both provided realistic and reasonable responses for both sites, although parametric analyses using reasonable variations in the major input parameters were still not sufficient to bracket all measures of the observed field responses. Both of these models can simulate post-triggering cyclic mobility behavior, and this was essential for computing reasonable responses after liquefaction was triggered. The results obtained using a third, much simpler model that counts stress cycles to determine when liquefaction is triggered, and then imposes a drop to the user-specified residual shear strength, was not able to approximate the post-triggering responses and consequently produced some unrealistic responses such as exaggerated base isolation effects and concentrations of strain within thin depth intervals. Sideras (2011) and Kramer et al. (2011) have similarly shown that the ability to model post-triggering cyclic mobility behavior is essential for realistic modeling of the seismic site response of liquefying soil profiles.

The differences between recorded and computed responses for these cases of liquefaction at downhole array stations are likely due to the combined influence of several factors, including the approximations and limitations associated with 1D site response analyses (e.g., absence of slopes, surface waves, embedded structures, lateral variability, lateral boundaries), site characterization, determination of soil properties, constitutive models, and numerical procedures. Kramer et al. (2011) present a detailed discussion of these and other factors, and subsequently note that recorded motions have almost always been affected by factors that the one-dimensional site response analyses were never intended to represent. In view of these considerations, the PM4-Sand model appears to have performed reasonably well as a component of the site response analyses of liquefaction at these down-hole arrays.

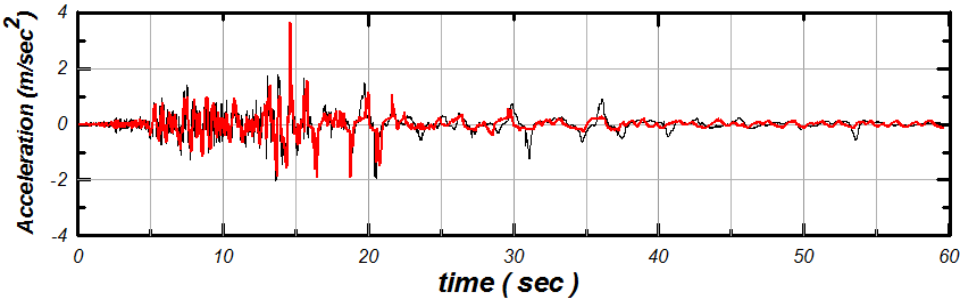

(a) Computed (red line) and recorded (black line) horizontal acceleration at the ground surface

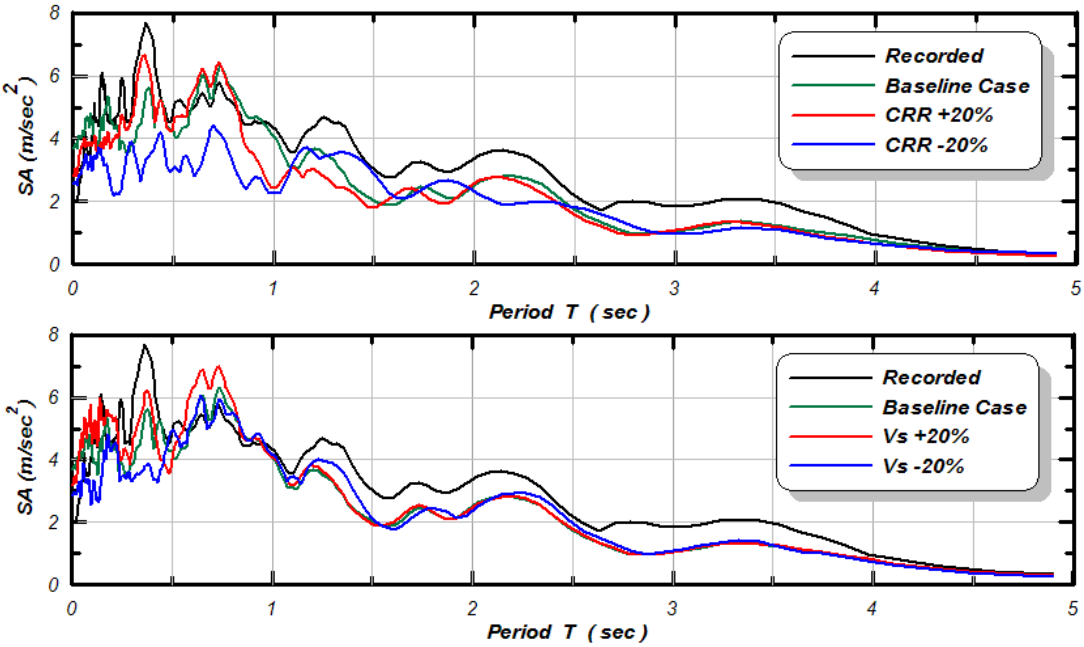

(b) Elastic response spectra (5% damping) for the horizontal motion at the ground surface

Fig. 8. Computed and recorded responses at the ground surface of the WLA site for the NS component of motion recorded in the 1987 Superstition Hills earthquake.

ANALYSES OF DYNAMIC CENTRIFUGE MODEL TESTS

Two-dimensional simulations of a dynamic centrifuge test involving liquefaction-induced lateral spreading were performed by Kamai and Boulanger (2011). The centrifuge test, SSK01, was performed to evaluate the effectiveness of geosynthetic drains for mitigating liquefaction of sands (Marinucci et al. 2008). The test was performed in a flexible shear beam container (0.8-m wide, 1.65-m long, 0.5-m deep) on the 9-m radius centrifuge at UC Davis. The test was performed at a centrifugal acceleration of 15 g and the results are presented in equivalent prototype units unless otherwise stated. The soil profile was constructed of two symmetrical sides, sloping at 3˚ towards a central channel. Both had a 5-m thick liquefiable layer of Nevada Sand (D_R=40%) overlain by a 1-m thick layer of clayey-silt (plasticity index, PI=13). Model-scale plastic drains were installed on one side of the centrifuge container prior to pluviation. The model was subjected to five main shaking events separated from each other by sufficient time for full dissipation of any excess pore water pressures. The five successive shaking events consisted of 20 uniform sinusoidal cycles at 2 Hz with single-amplitudes of 0.01, 0.03, 0.07, 0.11, and 0.3 g. They will be labeled in this paper as “shake 08”, “shake 09”, “shake 10”, “shake 11”, and “shake 12”, respectively (shakes 01-07 had amplitudes less than 0.02 g and did not lead to any significant development of pore pressures).

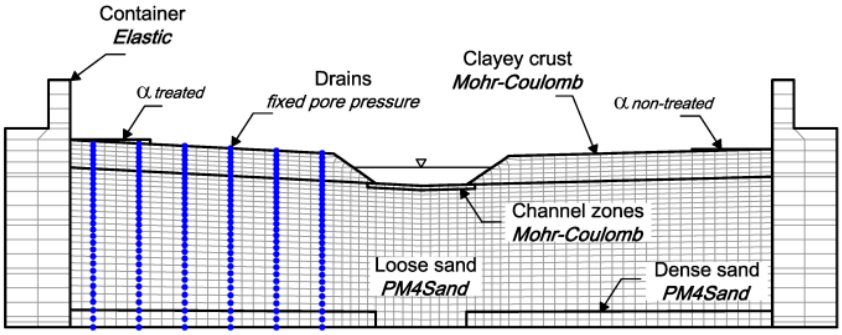

Fig.9 FLAC mesh, showing material models, location of drains and water table height.

The finite difference mesh and model geometry are shown in Fig. 9. The aluminum and rubber rings of the container are elastic materials, whose effective masses and properties were proportioned to achieve the correct ratio of container and soil masses (i.e., considering the out-of-plane thickness of the soil elements) and the correct fundamental frequency of the physical container. The clayey-silt crust is assigned a Mohr-Coulomb material model with measured values for the density and undrained strength. The sand layers, both loose (D_R=40%) and dense (D_R=80%), are modeled using PM4-Sand, calibrated to results of in-flight shear wave velocity measurements and cyclic strengths determined in laboratory element tests. The prefabricated vertical drains on the drain-treated side are simulated by fixing the pore pressures at vertical columns of nodes (see Fig. 9) to their hydrostatic value. This approximation of the drains will produce an over prediction of drainage with respect to the physical model test, but is sufficient for the purpose of this simulation, which is focused on the response of the non-treated side. The boundary between the soil elements and the container elements is modeled by a frictional interface that allows for relative movement of the soil with respect to the container elements. Vertical displacement of the container is restricted, and container nodes from both sides of the model are slaved to each other in the horizontal direction to represent the continuation of the container rings in three dimensions. Water within the central channel is modeled by applying the corresponding pressure to the channel nodes below the water table height. Shaking is applied by subjecting the bottom container nodes to the velocity time history that was measured at the bottom of the container in the centrifuge test. Rayleigh damping is set to 0.5% at a center frequency of 2 Hz, which is the dominant frequency of the input motion. Mesh node coordinates were updated after each time step (referred to as 'large deformation' in FLAC terminology) to account for changes in geometry due to deformations.

Simulations of the largest four shaking events were performed (amplitudes of 0.03 - 0.3 g) using the baseline set of properties, followed by a sensitivity study covering a range of cyclic strengths, hydraulic conductivities, and other parameters. The computed response shown in Fig. 10 for the untreated side of the model during shake 10 with the baseline parameters are illustrative of the overall results. This figure shows computed (in blue) and measured (in red) time series of crust acceleration, excess pore-pressure at mid-depth of the loose sand layer, lateral spreading at the ground surface, and vertical settlements at mid-slope. The numerical simulation is largely successful in capturing the trends and magnitudes of the response. The crust acceleration is slightly over-predicted and does not show quite the same de-amplification as observed in the centrifuge test. The simulation captures the fast accumulation of excess pore pressures and the early triggering of liquefaction throughout the profile, though dissipation rates are faster than in the test. A simulation with the permeability reduced by a factor of three produced dissipation rates that are in better agreement with measured pore pressure time histories, but over-predicts the lateral surface displacements. Lateral surface displacements are slightly over-predicted when compared to the centrifuge test measurements, whereas vertical settlements are under-predicted. The under-prediction of surface settlements is possibly because the cracking, slumping, and yielding of the crust material that was observed during the centrifuge test was not reproduced in the simulations. Overall, the computed dynamic responses are in reasonable agreement with the centrifuge test measurements, indicating that the primary features of soil behavior have been simulated reasonably well.

The contour plots in Figs. 11 and 12 show the computed values of the soil displacements (relative to the container base) and relative densities, respectively, at the end of shaking. The contours in Fig. 11 show significantly different deformation patterns in the treated and non-treated sides. On the non-treated side, there is a clear step in displacements across the upper row of sand elements just below the crust, such that the crust deformations are about twice as much as the sand deformations. The large crust displacements result in a gap opening between the non-treated crust and the container wall and significant flattening of the slope, as also observed in the centrifuge experiment. On the treated side, there is very little deformation and no concentration of deformations at the interface between the sand and the crust, in agreement with the experimental observations.

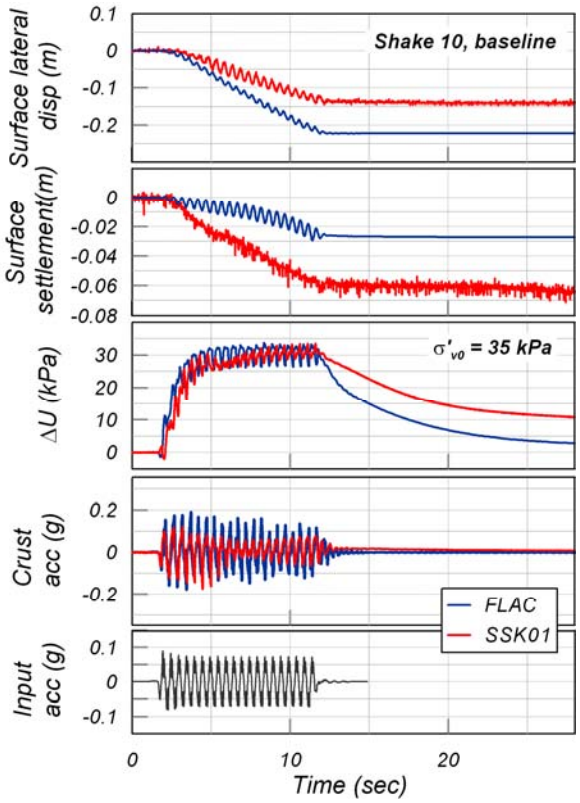

Fig. 10. Comparison of centrifuge test and simulation results for shake 10 with baseline properties.

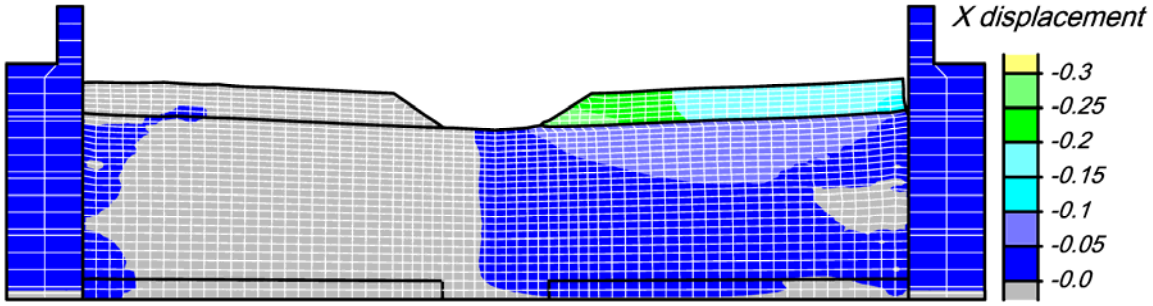

Fig. 11. Contours of horizontal displacements, relative to the container base, at end of shaking for the simulation of shake 10 with the baseline parameters.

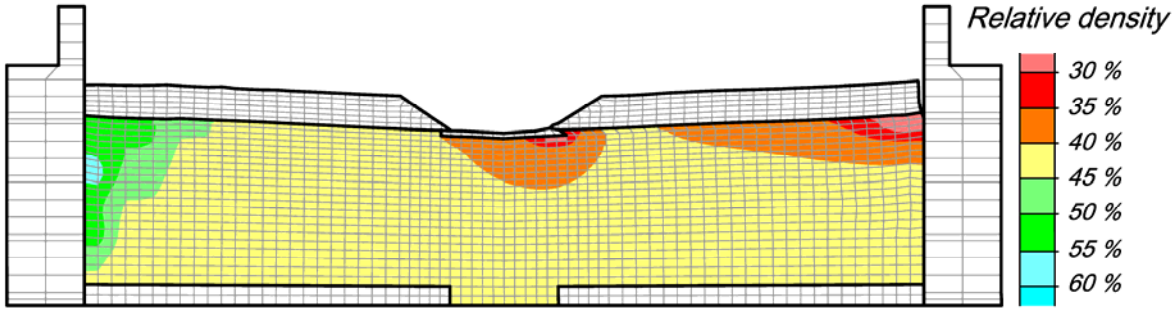

Fig. 12. Contours of relative density at the end of shaking for the simulation of shake 10 with the baseline parameters.

.

The spatial variations in relative densities, as shown in Fig. 12, are a consequence of the seepage patterns driven by the shaking induced excess pore water pressures. In particular, the general trend of upward pore water flow contributes to loosening of up to 8 sand elements at the top of the sand layer on the non-treated side, such that relative densities are reduced in local zones from their initial value of 40% to values of 30-35%. On the treated side, the upper sand elements do not experience significant loosening because the drains preclude the accumulation of water beneath the crust. The thickness of the loosening zone on the untreated side is a little less than 1 m, which is in good agreement with previous theoretical and experimental studies (Malvick et al. 2006; Malvick et al. 2008) as well as with the results of back analyses of the instrument arrays from this test (Kamai and Boulanger 2010). These other studies had identified loosening zones at the top of a confined liquefied sand layer that were about 0.6-m to 1.0-m thick, which is much greater than the expected thickness of any eventual localization (i.e., 10 or 20 grain diameters).

The general trends that were observed in the centrifuge test are successfully captured in the numerical simulations. The predicted surface deformations, pore pressure accumulation and dissipation patterns, and the distribution of strains throughout the profile agree well with the observations and measurements from the test. The effective mitigation of surface deformations by liquefaction drains, including the prevention of shear-strain localization at the sand/clay interface, is successfully simulated by the numerical model. It should be noted, however, that the representation of the drains as drainage walls in these simulations are expected to over-predict their effectiveness. Parametric analyses that enforced locally undrained conditions (no flow) or assumed small deformations both resulted in significantly poorer agreement with the experimental data, indicating the importance of including pore water flow and large deformation effects. Parametric analyses using a range of element thicknesses resulted in relatively minor differences. These results indicate that the primary physical mechanisms affecting the centrifuge model's responses are reasonably well simulated by the numerical platform and constitutive models used in these analyses.

CONCLUDING REMARKS

The stress-ratio controlled, critical state compatible, bounding surface plasticity model for sand presented herein was developed by progressively modifying the model by Dafalias and Manzari (2004) to improve its ability to approximate the stress-strain responses important to geotechnical earthquake engineering practice; in essence, the model was calibrated at the equation level to provide for better approximation of the trends observed in empirical correlations commonly used in practice in the U.S. Default values were provided for all but three primary input parameters: G_o which should be calibrated to the estimated or measured in-situ shear wave velocity, an apparent D_R which affects the peak drained and undrained strengths and the rate of strain accumulation during cyclic loading, and h_{po} which is used to calibrate to the estimated in-situ cyclic resistance ratio. The model was implemented as a user-defined material model for use with the commercial program FLAC (Itasca 2009). The implemented model was shown to provide reasonable approximations of desired element behaviors and to be relatively easy to calibrate.

Results were presented from initial applications of the model to numerical analyses of liquefaction effects. The one-dimensional site response analyses of liquefaction at the Wildlife Liquefaction Array during the 1987 Superstition Hills Earthquake produced reasonable agreement with the principle features of response, including the effects of post-liquefaction cyclic mobility behavior. The two-dimensional analyses of the dynamic centrifuge model test by Kamai et al. (2008) also produced reasonable agreement with the recorded responses, including the surface deformations, the accumulation and dissipation of pore pressures, the distribution of strains throughout the profile, and the effectiveness of the drains in preventing shear-strain concentrations at the sand/clay interface. These results indicate that the primary physical mechanisms affecting the observed liquefaction-related responses are reasonably well simulated by the numerical platform and constitutive models used in these analyses.

ACKNOWLEDGMENTS

Funding for portions of this research was provided the U.S. Geological Survey through Award G09AP00121. Support for the first author was provided by the 2008 International Fulbright Science and Technology Award from the Institute of International Education and the U.S. Department of State. Richie Armstrong provided the FLAC model for the centrifuge container. The centrifuge test was performed in collaboration with Ellen Rathje, Antonio Marinucci, Seiji Kano, Carolyn Conlee, and Patricia Gallagher with funding from NSF Award No. CMS-0530478. The authors appreciate the above support and assistance.

REFERENCES

Andrus, R. D., and K. H. Stokoe [2000], "Liquefaction resistance of soils from shear-wave velocity", J. Geotechnical and Geoenvironmental Eng., ASCE 126(11), 1015–025.

Bolton, M. D. [1986], "The strength and dilatancy of sands", Geotechnique 36(1), 65–78.

Boulanger, R. W. [2010], "A sand plasticity model for earthquake engineering applications", Report No. UCD/CGM-10-01, Center for Geotechnical Modeling, Department of Civil and Environmental Engineering, University of California, Davis, California.

Boulanger, R. W. [2003], "Relating K_α to relative state parameter index", J. Geotechnical and Geoenvironmental Eng., ASCE 129(8), 770–73.

Boulanger, R. W. and Idriss, I. M. (2004). "State normalization of penetration resistances and the effect of overburden stress on liquefaction resistance." Proc., 11th International Conference on Soil Dynamics and Earthquake Engineering, and 3rd International Conference on Earthquake Geotechnical Engineering, D. Doolin et al., eds., Stallion Press, Vol. 2, 484-491.

Byrne, P. M., S. S.Park, M. Beaty, M. K. Sharp, L. Gonzalez, and T. Abdoun [2004], "Numerical modeling of liquefaction and comparison with centrifuge tests", Canadian Geotechnical Journal, 41 (2), 193-211.

Dafalias, Y. F., and M. T. Manzari [2004], "Simple plasticity sand model accounting for fabric change effects", Journal of Engineering Mechanics, ASCE, 130(6), 622-634.

Electric Power Research Institute [1993], Guidelines for site specific ground motions, Rept. TR-102293, 1-5, Palo Alto, California.

Holzer, T. L., and T. L. Youd [2007], "Liquefaction, Ground Oscillation, and Soil Deformation at the Wildlife Array, California", Bull. Seism. Soc. Am., Vol. 97, No. 3, pp. 961-976.

Idriss, I. M., and R. W. Boulanger [2008], Soil liquefaction during earthquakes, Monograph MNO-12, Earthquake Engineering Research Institute, Oakland, CA, 261 pp.

Itasca [2009], FLAC – Fast Lagrangian Analysis of Continua, Version 6.0, Itasca Consulting Group, Inc., Minneapolis, Minnesota.

Kamai, R., and R. W. Boulanger [2011], "Numerical simulations of a centrifuge test to study void-redistribution and shear localization effects." 8th Intl. Conference on Urban Earthquake Engineering, Tokyo Institute of Technology, Tokyo, Japan, 455-459.

Kamai, R. and R. W. Boulanger [2010], "Characterizing localization processes during liquefaction using inverse analyses of instrumentation arrays", Meso-Scale Shear Physics in Earthquake and Landslide Mechanics. Y. H. Hatzor, J. Sulem and I. Vardoulakis. The Netherlands, CRC Press/.Balkema: 219-238.

Kamai, R., S. Kano, C. Conlee, A. Marinucci, R. W. Boulanger, E. Rathje, G. Rix, and R. Howell [2008], "Evaluation of the effectiveness of prefabricated vertical drains for liquefaction remediation - centrifuge data report for SSK01", Report No. UCD/CGM-08/01, Center for Geotechnical Modeling, Dept. of Civil and Environmental Engineering, University of California, Davis, California.

Kramer, S. L., A. J. Hartvigsen, S. S. Sideras, and P. T. Ozener [2011], "Site Response Modeling in Liquefiable Soil Deposits", 4th IASPEI / IAEE Intl. Symposium, Effects of Surface Geology on Seismic Motion, Univ. of California, Santa Barbara, August 23-26.

Liu, A. H., J.P. Stewart, N. A. Abrahamson, and Y. Moriwaki, Y. [2001], "Equivalent number of uniform stress cycles for soil liquefaction analysis", J. Geotechnical and Geoenvironmental Engineering, ASCE 127(12), 1017-1026.

Malvick, E. J., B. L. Kutter, and R. W. Boulanger [2008], "Postshaking shear strain localization in a centrifuge model of a saturated sand slope", Journal of Geotechnical and Geoenvironmental Engineering 134(2): 164-174.

Malvick, E. J., B. L. Kutter, R. W. Boulanger, and R. Kulasingam [2006], "Shear localization due to liquefaction-induced void redistribution in a layered infinite slope", Journal of Geotechnical and Geoenvironmental Engineering 132(10): 1293-1303.

Marinucci, A., E. Rathje, S. Kano, R. Kamai, C. Conlee, R. Howell, R. W. Boulanger, and P. Gallagher [2008], "Centrifuge Testing of Prefabricated Vertical Drains for Liquefaction Remediation", Geotechnical Earthquake Engineering and Soil Dynamics IV, D. Zeng, M. Manzari, and D. Hiltunen, eds., Geotechnical Special Publication No. 181, ASCE, NY.

Sideras, S. S. [2011], "One-dimensional effective stress response analysis of liquefiable soil profiles", Masters thesis, University of Washington, 207 pp.

Ziotopoulou, K. [2010], "Evaluating model uncertainty against strong motion records at liquefiable sites", Masters thesis, University of California, Davis, 294 pp.